

Provided for non-commercial research and education use.
Not for reproduction, distribution or commercial use.



This article appeared in a journal published by Elsevier. The attached copy is furnished to the author for internal non-commercial research and education use, including for instruction at the authors institution and sharing with colleagues.

Other uses, including reproduction and distribution, or selling or licensing copies, or posting to personal, institutional or third party websites are prohibited.

In most cases authors are permitted to post their version of the article (e.g. in Word or Tex form) to their personal website or institutional repository. Authors requiring further information regarding Elsevier's archiving and manuscript policies are encouraged to visit:

<http://www.elsevier.com/copyright>



Multi-armed spirals and multi-pairs antispirals in spatial rock–paper–scissors games

Luo-Luo Jiang^{a,b,*}, Wen-Xu Wang^{c,d}, Ying-Cheng Lai^{c,e}, Xuan Ni^c

^a College of Physics and Electronic Information Engineering, Wenzhou University, Wenzhou 325035, China

^b College of Physics and Technology, Guangxi Normal University, Guilin, Guangxi 541004, China

^c School of Electrical, Computer and Energy Engineering, Arizona State University, Tempe, AZ 85287, USA

^d Department of Physics, Beijing Normal University, Beijing 100875, China

^e Department of Physics, Arizona State University, Tempe, AZ 85287, USA

ARTICLE INFO

Article history:

Received 12 January 2012

Received in revised form 17 May 2012

Accepted 30 May 2012

Available online 4 June 2012

Communicated by C.R. Doering

Keywords:

Spiral

Antispiral

Rock–paper–scissors game

Nonlinear system

ABSTRACT

We study the formation of multi-armed spirals and multi-pairs antispirals in spatial rock–paper–scissors games with mobile individuals. We discover a set of seed distributions of species, which is able to produce multi-armed spirals and multi-pairs antispirals with a finite number of arms and pairs based on stochastic processes. The joint spiral waves are also predicted by a theoretical model based on partial differential equations associated with specific initial conditions. The spatial entropy of patterns is introduced to differentiate the multi-armed spirals and multi-pairs antispirals. For the given mobility, the spatial entropy of multi-armed spirals is higher than that of single armed spirals. The stability of the waves is explored with respect to individual mobility. Particularly, we find that both two armed spirals and one pair antispirals transform to the single armed spirals. Furthermore, multi-armed spirals and multi-pairs antispirals are relatively stable for intermediate mobility. The joint spirals with lower numbers of arms and pairs are relatively more stable than those with higher numbers of arms and pairs. In addition, comparing to large amount of previous work, we employ the no flux boundary conditions which enables quantitative studies of pattern formation and stability in the system of stochastic interactions in the absence of excitable media.

© 2012 Elsevier B.V. All rights reserved.

Formation of self-organized pattern is a fundamental aspect of physical and biological systems out of equilibrium. Spiral waves are quite common in a variety of excitable systems and population dynamics, such as Belousov–Zhabotinsky reaction [1,2], the cardiac tissue [3], insect population dynamics [4] and cyclically competing populations with mobility [5]. Spiral waves play significant roles in the dynamics of excitable systems, e.g., in heart disease, such as arrhythmia and fibrillation, which lead to death [3,6,7]. Spiral waves are important in population dynamics as well. In particular, biodiversity in cyclically competing populations with stochastic interactions can be maintained and stabilized by entangled moving spiral waves [5,8]. The coexistence of two or more spirals may form multi-armed spiral and antispiral waves. These interesting joint spirals have been extensively studied in excitable systems theoretically and experimentally [9–14]. However, in the population dynamics in the presence of stochastic processes, multi-armed spirals and multi-pairs antispirals among entangled spirals is rarely studied and far from being well understood. There are two impor-

tant open questions associated with these waves: Are they able to be generated through stochastic interactions and how is their stability? The purpose of this Letter is to address these questions in the framework of cyclic competing games with mobile individuals.

Non-hierarchical cyclic competitions have been observed in a number of real ecosystems, ranging from colicinogenic microbes competition to mating strategies of side-blotched lizards in California [15–19], as well as human sociality in terms of public goods games [20–22]. The essential features of such competition can be captured by the childhood game “rock–paper–scissors” (RPS). In the game, species coexistence, as the key factor for maintaining biodiversity, has been given much attention, especially for the conditions that ensure species coexistence [23–31]. Both laboratory experiment and theoretical model have revealed that spatial structure by confining local interaction is necessary for stabilizing species coexistence [19]. Otherwise, stochastic effect and external perturbation can easily ruin biodiversity. Quite recently, individual mobility has been incorporated in the spatial RPS game [5,8,32,33]. It has been found that individual mobility induces entangled moving spiral waves which preclude species from extinction [5]. The stochastic game has been casted into a set of partial differential equations by a continuous approximation [8]. In this Letter, we investigate the origin of multi-armed spiral waves and multi-pairs

* Corresponding author at: College of Physics and Electronic Information Engineering, Wenzhou University, Wenzhou 325035, China. Tel.: +86 18267788986.

E-mail address: jiangluolu@gmail.com (L.-L. Jiang).

antispiral waves on the basis of the spatial RPS game with mobile individuals, which is unaddressed prior to our work. We find that the joint spiral waves can spontaneously arise due to the interaction of neighboring spirals and the type of the joint spirals is determined by the position and rotational directions of neighboring spirals. In particular, we discover a general set of seeds of species distribution, which is capable of producing multi-armed spirals with a finite number of arms and antispirals with finite number of pairs. The diverse patterns generated from stochastic simulations are reproduced by solving a set of partial differential equations from specific initial conditions. We have also discussed the stability of the joint spiral waves with respect to individual mobility.

We consider the spatial RPS game proposed in Ref. [5]. Nodes of a $L \times L$ square lattice with no flux boundary conditions sustain mobile individuals belonging to one of the three species, A , B and C . Each node can either host one individual of a given species or it can be vacant. Vacant sites, denoted by \otimes , are also the so-called resource sites where individuals of species reproduce offspring. The dynamical process can be described as following:



where \odot denotes any species or vacant sites. These reactions describe three processes, i.e. competition, reproduction and exchange, occurring only between neighboring nodes. In reaction (1), species A eliminates species B at a rate 1, whereby the node previously hosting species B becomes vacant. In the same manner species B can kill species C , and species C can kill species A , thus forming a closed loop. In reaction (2), individuals place an offspring to a neighboring vacant node \otimes at a rate 1. Reaction (3) defines exchange process where an individual exchanges its position with an individual belonging any species or an empty site at a rate γ . According to the theory of random walks [34], mobility of individuals M is defined as: $M = \gamma/2N$, where $N = L \times L$ and M represents the typical area explored by one mobile individual per unit time.

We apply stochastic algorithm developed by Gillespie to simulate the system's evolution [35], where the occurring probabilities of reactions are determined by their rates. In our model, competition and reproduction occur with probability $1/(\gamma + 2)$, whereas exchange (moving) occurs with probability $\gamma/(\gamma + 2)$. At each step, an individual is randomly selected to interact with one randomly selected neighboring site. In one time step, all individuals are selected once on average.

A critical value $M_c = (4.5 \pm 0.5) \times 10^{-4}$ of mobility has been identified in Ref. [5]. Below M_c , three subpopulations can stably coexist in the form of moving spiral waves; while above M_c , the wave length of spirals exceeds the size of underlying lattice and biodiversity is lost. Here, we focus on the biodiversity region for $M < M_c$. In this region, by carrying out sufficient stochastic simulations from random initial distributions of species, we found there is chance to observe both multi-armed spirals and multi-pairs antispirals, as shown in Fig. 1(b) and (e). For different specific initial conditions (see Fig. 2(b) and (c) for details), a two-armed spiral and an one-pair antispiral can be reproduced, as shown in Fig. 1(a) and (c) respectively, which are qualitatively the same as the marked patterns in Fig. 1(b). In addition, as shown in Fig. 1(a) and (c) respectively, a one-armed spiral and a two-pairs antispiral emerge from special initial conditions (see Fig. 2(d) and (e) for details), which are observed in Fig. 1(e). We also found that these patterns can last for relative long time and then they may disappear or transform to single armed spirals with the initial conditions of species randomly distributing on the lattice. In the

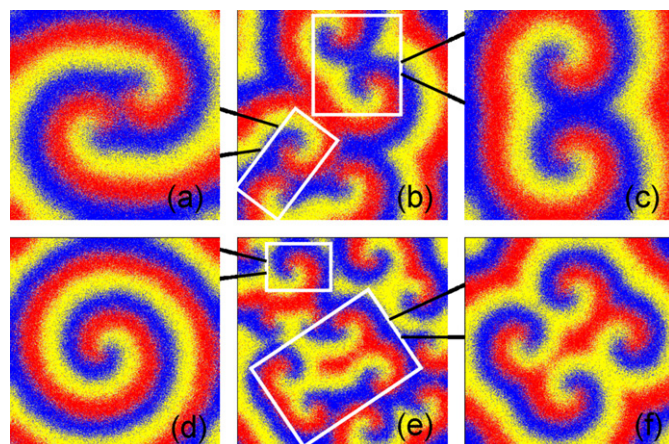


Fig. 1. (Color online.) Spatial patterns in RPS game for $M = 5.0 \times 10^{-5}$. Panels (b) and (e) are obtained from random distribution of three species initially. In panels (a), (c), (d), and (f), the system starts from specific seed distributions of three species. The marked local patterns in (b) can be reproduced from specific initial conditions, as shown in (a) and (c). The marked local patterns in (e) can be generated as well, as shown in (d) and (f). $L = 512$ for all panels.

multi-armed spirals, the arms rotate in the same direction with the same speed, resulting exclusively from stochastic interactions among neighboring individuals. In the antispirals, the two spirals of a pair rotate with the same speed but in reverse directions. The identical rotational speed of sub-spirals in the waves ensures their stable existence. It is noteworthy mentioning that the patterns in Fig. 1 are obtained from no flux boundary conditions, and we also examine the phase transition of system from biodiversity to uniformity with no flux boundary conditions. As shown in Fig. 2(a), a critical mobility M_c emerges at 4.5×10^{-4} , which is the same as the result of periodic boundary conditions in Ref. [5].

It is interesting to find that the multi-armed spirals and multi-pairs antispirals can arise from some specific distribution of three subpopulations. As shown in Figs. 2(b) and 2(c), square, triangle and circle symbols stand for a small amount of three subpopulations which are placed on a lattice with no flux boundary condition. Other sites of the lattice are left empty. In the early stage, each pile of individuals expand due to reproduction. After the boundaries of different species encounter, populations begin to rotate because of the cyclic competition. Finally, after the systems reaching a non-equilibrium steady state, a two-armed spiral and a one-pair antispirals emerge. Let's see Fig. 2(b), the six pile of species placed around a circle are in the order $A, B, C, A, B,$ and C . The six piles can be separated into two groups, each of which contains three species. During the evolution, each group form an arm. Due to the spatial symmetry of the two group, the wave length, rotation speeds and directions of the two arms are the same, giving rise to a steady two-armed spiral (Fig. 1(a)). In contrast, to generate antispirals, we need to place a finite number of species at the center of a circle and the other two species around the circle (Fig. 2(c)), leading to a steady one-pair antispiral (Fig. 1(c)).

By extending the simple configuration in Fig. 2(b) and (c), we discover a general route to generate multi-armed spirals with a finite number of arms and antispirals with a finite number of pairs. To articulate the method, we should define the basic cell in the initial distribution of species. As shown in Fig. 2(d), the cell of multi-armed spirals is composed of three species in the order A, B and C . The cell of antispiral contains two species except the central species. The central species can be a finite number, but once the central species is fixed, the cell is fixed as well. For the multi-armed spirals, the number of arms is determined by the number of cells. In general, one arm can be formed by one cell, so that by adjusting the number of cells, one can obtain multi-armed spirals

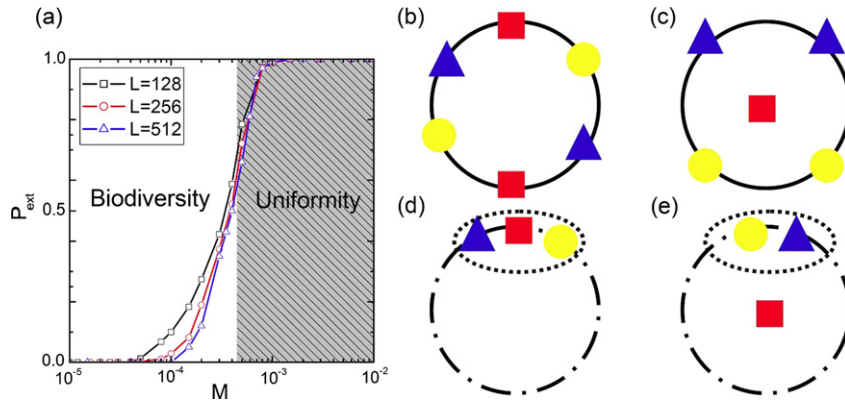


Fig. 2. (Color online.) In panel (a), extinction probability P_{ext} as a function of mobility M . Seed distribution of species for producing (b) two-armed spiral, (c) one pair antispiral, (d) multi-armed spirals with a finite number of arms and (e) antispirals with a finite number of pairs. Both the solid circle and the dash-dot circle denote seeds distribute in the round manner in panels (b), (c), (d), (e). In addition, dash-dot circle in panels (d) and (e) means the number of seeds can be extended, and the number of arms (pairs) of multi-armed spirals (multi-pairs antispirals) equals to the number of dash rings where seeds distribute in such special manner.

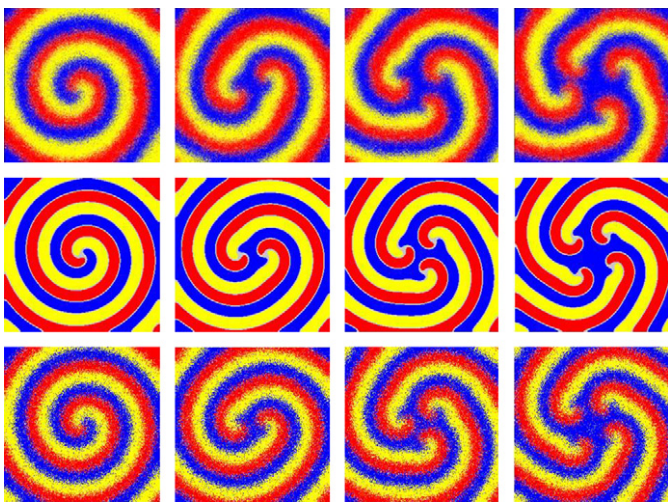


Fig. 3. (Color online.) Multi-armed spirals with one, two, three and four arms by stochastic simulations (top panels) and by solving PDEs (medial and bottom panels). It is worthy mentioning that both patterns in medial and bottom panels are determined by the densities of three species on all the spatial sites. In the bottom rows, the site i is denoted by the color of species A with probability $a(\mathbf{r}, t)/[a(\mathbf{r}, t) + b(\mathbf{r}, t) + c(\mathbf{r}, t)]$, by B 's color with probability $b(\mathbf{r}, t)/[a(\mathbf{r}, t) + b(\mathbf{r}, t) + c(\mathbf{r}, t)]$, and by C 's color with probability $c(\mathbf{r}, t)/[a(\mathbf{r}, t) + b(\mathbf{r}, t) + c(\mathbf{r}, t)]$, where $a(\mathbf{r}, t)$, $b(\mathbf{r}, t)$, $c(\mathbf{r}, t)$ are rate of species A , B , and C respectively. As shown in the medial rows, patterns are obtained in a deterministic way, where the site i is denoted by the color of species A if $a(\mathbf{r}, t)$ is the largest among rates of species. In this way, colors of species B , C can be obtained, and the empty site is denoted by gray color. The parameters are $M = 5.0 \times 10^{-5}$ for top rows and $D = 5.0 \times 10^{-5}$ for medial and bottom rows, $L = 512$.

with any number of arms. For the antispiral, the number of cells equals the number of antispiral pairs. One-pair antispirals is different from this regulation, as shown in Fig. 2(c). Two cells with reverse orders are required to create one-pair antispirals, as shown in Fig. 2(e). Stochastic simulation results from a set of seed distribution with different numbers of cells are shown in top panels of Fig. 3 for multi-armed spirals and in top panels of Fig. 4 for multi-pairs antispirals, respectively. The patterns justify the generate route to producing multi-armed spirals and multi-pairs antispirals.

It is noteworthy that a large number of arms or pairs is not stable because of the stochastic effect. Although all arms or pairs can be formed, after a while, some arms or pairs will be intruded by neighboring arms or pairs and disappear. The no flux boundary conditions are also necessary to generate the waves. In contrast, for periodic boundary conditions, the joint spirals in global scale

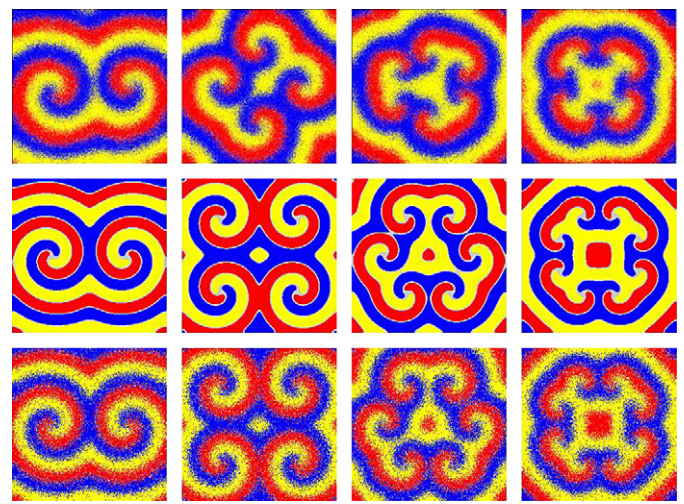


Fig. 4. (Color online.) Antispirals with one, two, three and four pairs by stochastic simulations (top panels) and by solving PDEs (medial and bottom panels). The color of patterns and the parameters are the same as in Fig. 3.

will be destroyed and break into small spirals. The symmetry of the distribution of cells sustains the stability of multi-armed spirals and multi-pairs antispirals, and better symmetry lead to more stable waves. The radii of the circle and the number of individuals in each pile do not affect the wave patterns.

The patterns generated by stochastic simulations can be predicted theoretically by a set of partial differential equations (PDEs). As derived in the works of Reichenbach et al. [5,8], starting from rate equations and applying the continuous approximation, we have

$$\begin{aligned} \partial_t a(\mathbf{r}, t) &= D \nabla^2 a(\mathbf{r}, t) + a(\mathbf{r}, t)(1 - \rho) - c(\mathbf{r}, t)a(\mathbf{r}, t), \\ \partial_t b(\mathbf{r}, t) &= D \nabla^2 b(\mathbf{r}, t) + b(\mathbf{r}, t)(1 - \rho) - a(\mathbf{r}, t)b(\mathbf{r}, t), \\ \partial_t c(\mathbf{r}, t) &= D \nabla^2 c(\mathbf{r}, t) + c(\mathbf{r}, t)(1 - \rho) - b(\mathbf{r}, t)c(\mathbf{r}, t), \end{aligned} \quad (4)$$

where $a(\mathbf{r}, t)$, $b(\mathbf{r}, t)$ and $c(\mathbf{r}, t)$ are the densities of species A , B , C at position \mathbf{r} and time t , $\rho = a(\mathbf{r}, t) + b(\mathbf{r}, t) + c(\mathbf{r}, t)$ is the local species density and $1 - \rho$ denotes the density of empty sites. Eulerian difference method and Runge-Kutta method are applied to solve the PDEs. The initial conditions are $a(\mathbf{r}) = b(\mathbf{r}) = c(\mathbf{r}) = 0$ for all spatial coordinate \mathbf{r} except the initial seed species in Fig. 2. In the coordinate of seed, one species' density is one and the others are zero. The patterns generated by numerically solving the PDEs are exhibited in the medial and bottom rows of Figs. 3 and 4 for

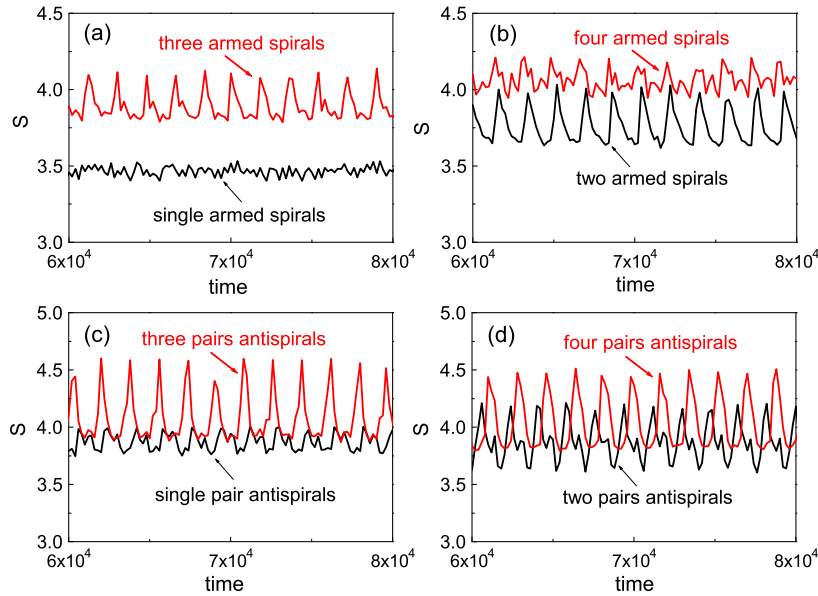


Fig. 5. (Color online.) The spatial entropy varying with time at $D = 5.0 \times 10^{-5}$ for multiple armed spirals and antispirals obtained from PDE method, single armed and three armed spirals in (a), two armed and four armed spirals in (b), two armed and three pairs antispirals in (c), four armed and four pairs antispirals in (d). The pattern formations are shown in bottom panels of Figs. 3 and 4 respectively. Initial conditions are shown in Fig. 2(b), (c), (d) and (e). $L = 512$ for all panels.

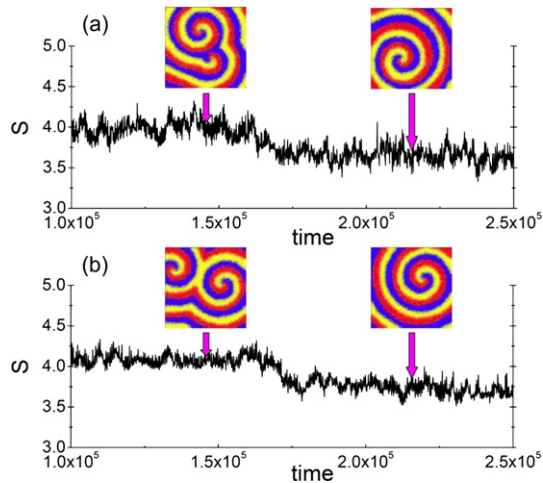


Fig. 6. (Color online.) The spatial entropy evolves with time at $M = 4.0 \times 10^{-5}$ for two armed spirals in panel (a) and single pair antispirals in panel (b). It is notable that both two armed spirals and one pair antispirals become single armed spirals in the end, and patterns in panel (a) and panel (b) obtained at time of 1.45×10^5 and 2.15×10^5 respectively. Initial conditions are shown in Fig. 2(b), (c), (d) and (e). $L = 512$ for all panels and one time step is defined as all individuals are selected once.

multi-armed spirals and multi-pairs antispirals, respectively. The patterns obtained from PDEs are in good agreement with results of stochastic simulations. The colors of patterns obtained by PDEs are determined by the densities of three species on all the spatial sites. As shown in bottom rows in Figs. 3 and 4, at a finite number of location (\mathbf{r}) and time t , the site i is denoted by the color of species A with probability $a(\mathbf{r}, t)/[a(\mathbf{r}, t) + b(\mathbf{r}, t) + c(\mathbf{r}, t)]$, by B 's color with probability $b(\mathbf{r}, t)/[a(\mathbf{r}, t) + b(\mathbf{r}, t) + c(\mathbf{r}, t)]$, and by C 's color with probability $c(\mathbf{r}, t)/[a(\mathbf{r}, t) + b(\mathbf{r}, t) + c(\mathbf{r}, t)]$, where $a(\mathbf{r}, t)$, $b(\mathbf{r}, t)$, $c(\mathbf{r}, t)$ are rate of species A , B , and C respectively. A deterministic method is used to obtain patterns by PDEs. As shown in the medial rows of Figs. 3 and 4, the site i is denoted by the color of species A if $a(\mathbf{r}, t)$ is the largest among rates of species. In this way, colors of species B , C can be obtained, and the empty site is denoted by gray color.

To quantitatively investigate the emergence of multi-armed spirals and multi-pairs antispirals, we define the spatial entropy of patterns according to Shannon entropy [36]:

$$S = - \sum_{i=1}^z p_i \ln(p_i), \quad (5)$$

where z is the number of the clusters formed by individuals of the same species and p_i is the probability of the cluster with size of x_i , $p_i = x_i/N$. Here, the size x_i is the number of individuals of the same species in cluster i . In the simulation, the size of cluster x_i is the number of individuals of the same species in the same cluster, and the probability of the cluster with size x_i is x_i/N , where N is the size of the system. The spatial entropy can then be calculated according to Eq. (5), and $\ln(p_i)$ is the natural logarithm for p_i . For the PDE method, the spatial entropy is calculated according to colors patterns which are quantified by the densities of three species on all the spatial sites, as shown in bottom rows in Figs. 3 and 4. In this regard, the spatial entropy measures the disorder degree of spatial patterns in the system. For the extreme case, $x_i = N$, e.g. the system is predominated by one species, there are only one cluster in the system, and the entropy equals to zero. In the case of three species randomly distributed on lattice of $N = 512 \times 512$, the spatial entropy tends to be $-\ln(1/N) \approx 12.5$. Given $N = 512 \times 512$, the spatial entropy of pattern formation ranges from 0 to 12.5. Therefore, we can quantitatively study disorder of spatial patterns in terms of entropy. Fig. 5 shows spatial entropy of multi-armed spirals and multi-pairs antispirals as function of time with PDE method. Average values of spatial entropy are 3.4, 3.7, 3.8, and 4.0 for one-armed, two-armed, three-armed, and four-armed spirals respectively, while average values of spatial entropy are 3.8 for both one-pair and two-pairs antispirals, 4.0 for both three-pair and four-pairs antispirals. One can find that the spatial entropy of single spirals is smaller than that of multi-armed spirals and multi-pairs antispirals. In addition, the transition time is about 12000 time steps from the two armed spirals to the single armed spirals and about 16000 time steps from the one pair antispirals to the single armed spirals.

Since multi-armed spirals and multi-pairs spirals are unstable at too small or large mobility, without loss of generality, we investigate the evolution of pattern and spatial entropy at

$M = 4.0 \times 10^{-5}$ with stochastic algorithm. Fig. 6 shows the spatial entropy evolving with Monte Carlo (MC) time for two armed spirals and one pair antispirals which transform to the single armed spirals, and one can find that the two armed spirals and one pair antispirals emerge in the system at beginning, as shown in left insets of Figs. 6(a) and 6(b) respectively, while after long time evolving both two armed spirals and one pair antispirals become the single armed spirals, as shown in right insets of Figs. 6(a) and 6(b) respectively. The transition time is about 12000 time steps from the two armed spirals to the single armed spirals and about 16000 time steps from the one pair antispirals to the single armed spirals. In addition, the spatial entropy reduces after the transformation.

Finally, we examine the stability of spirals and antispirals with respect to the individual mobility M . The stability denotes the probability that spirals or antispirals are maintained after the patterns emerge. Each probability of the stability is obtained from 100 different independent realizations. For example, for given M and L , if there are 50 times that the single armed spirals survive, the stability of single armed spirals is 0.5. Without loss of general, if the value of stability is higher than 0.5, the pattern is regarded as stable, otherwise the pattern is regarded as unstable. Therefore, we calculate the stability of spirals and antispirals from 100 independent realizations, as shown in Fig. 7, in the stable region in the parameter space of M , the value of stability of all patterns are higher than 0.5. The shadow and gray regions in Fig. 7(a) denote one-armed spirals and two-armed spirals emerging stably in the system, respectively. There are three regions: for small values of M , $M < 1.0 \times 10^{-5}$, both single spiral and two-armed spiral break into a number of small spirals; for large values of M , $M > 1.0 \times 10^{-3}$, biodiversity is lost and spirals disappear; for intermediate values of M , both spirals survive. The single spiral is more stable than the two-armed spiral and the latter can transform to the former. The similar phenomenon is also observed for multi-pairs antispirals. As shown in Fig. 7(b), one-pair and two-pairs antispirals exist stably in the blue (dark) and green (light) region respectively. There exhibit three regions and the one-pair is more stable than the two-pair, similar to the multi-armed spirals. The top panels of Fig. 7 demonstrate that at the boundaries of three regions, the two-pair antispirals reduces to single spiral.

Spatiotemporal patterns have been investigated extensively, ranging from chemical reactions on catalytic surfaces to propagating signals in aggregating microorganisms [37]. It is found that patterns in excitable media emerge primarily due to the instabilities induced by the interplay between the fast excitatory and slow recovery variables. This kind of mechanism explain well the multi-armed spirals and antispirals emerging in the Belousov–Zhabotinsky (BZ) reaction [10] as well as cardiac substrate [11], and aggregating amoeba *D. discoideum* [12]. However, multi-armed spirals and multi-pairs antispirals in our systems emerge because of cyclic interaction in populations of three species with the same mobility. In this Letter, we have explored the origin and stability of multi-armed spirals and multi-pairs antispirals in the spatial rock–paper–scissors game with mobile individuals. The two types of joint spirals are naturally observed by stochastic simulations. We have discovered a set of seed distributions of species, which is able to produce multi-armed spirals and multi-pairs antispirals with a finite number of arms and anti-pairs. The availability of the seed for producing the waves are justified by both stochastic simulations and a theoretical model described by a set of partial differential equations. The patterns obtained by PDEs are consistent with numerical patterns. We have also discussed the stability of multi-armed spirals and multi-pairs antispirals depending on the individual mobility. We found that in the intermediate mobility, both waves are relatively stable, whereas for low mobility, the spirals in the global scale breaks into small spirals and for high

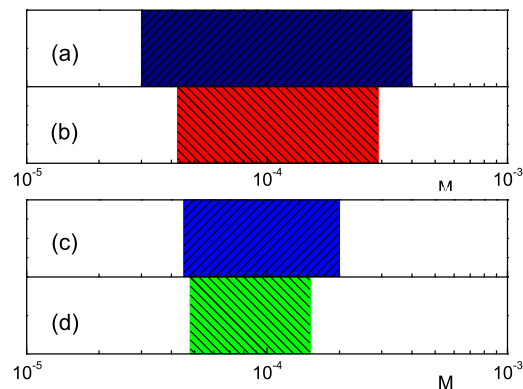


Fig. 7. (Color online.) The navy-blue (dark) and red (light) region indicate emerging stably of one- and two-armed spirals respectively in panel (a) and panel (b). The blue (dark) and green (light) region show appearing stably of one- and two-pairs antispirals respectively in panel (c) and (d). Results are obtained from 100 different independent realizations, $L = 512$.

mobility, spirals disappear due to the loss of biodiversity. We have also found that large numbers of arms or anti-pairs weaken the stability of the joint spirals and the joint spirals with larger numbers of arms or anti-pairs can transform to less numbers of arms or anti-pairs. It is noteworthy that our model is quite simple and only focuses on the competitions among species, such that the model is unable to capture and reproduce all dynamical behaviors in real ecosystems. For example, in our model the death of individuals can be exclusive induced by competitions among different species. However, the natural death mechanism is lacking, which prevents extinctions of single species in a small patch, in opposite to the reality that any small colony dies [38,39]. In addition, due to the simplification of migration in our work, the current results of biodiversity inhibited by migration is quite different from the reported results in literature that there exist optimal migration rates to facilitate biodiversity [40] and cooperation [41] in real systems.

Acknowledgements

The authors would like to thank Dr. Liang Huang for his helpful discussion in preparing this Letter. LLJ and WXW were supported by the National Natural Science Foundation of China (Grant Nos. 11047012 and 11105011). WXW and YCL were supported by AFOSR under Grant No. FA9550-09-1-0260. YCL was supported by AFOSR under Grant No. FA9550-10-1-0083, by NSF under Grants No. CDI-1026710 and No. BECS-1023101.

References

- [1] A.N. Zaikin, A.M. Zhabotinsky, *Nature* 225 (1970) 535.
- [2] A.T. Winfree, *Science* 175 (1972) 634.
- [3] J.M. Davidenko, A.V. Pertsov, R. Salomonsz, W. Baxter, J. Jalife, *Nature* 355 (1992) 349.
- [4] M.P. Hassell, H.N. Comins, R.M. May, *Nature* 353 (1991) 255.
- [5] T. Reichenbach, M. Mobilia, E. Frey, *Nature* 448 (2007) 1046.
- [6] R.A. Gray, A.M. Pertsov, J. Jalife, *Nature* 392 (1998) 75.
- [7] H. Zhang, Z. Cao, N.J. Wu, H.P. Ying, G. Hu, *Phys. Rev. Lett.* 94 (2005) 188301.
- [8] T. Reichenbach, M. Mobilia, E. Frey, *J. Theor. Biol.* 254 (2008) 368.
- [9] K.I. Agladze, V.I. Krinsky, *Nature* 296 (1982) 424.
- [10] V.K. Vanag, I.R. Epstein, *Science* 294 (2001) 835.
- [11] N. Bursac, F. Aguel, L. Tung, *Proc. Natl. Acad. Sci. USA* 101 (2004) 15530.
- [12] B. Vasiev, F. Siegert, C. Weijer, *Phys. Rev. Lett.* 78 (1997) 2489.
- [13] C. Zemplin, K. Mukund, M. Wellner, R. Zaritsky, A. Pertsov, *Phys. Rev. Lett.* 95 (2005) 098302.
- [14] L.-Y. Deng, H. Zhang, Y.-Q. Li, *Phys. Rev. E* 81 (2010) 016204.
- [15] T.L. Czárán, R.F. Hoekstra, L. Pagie, *Proc. Natl. Acad. Sci. USA* 99 (2002) 786.
- [16] B. Sinervo, C.M. Lively, *Nature* 380 (1996) 240.
- [17] C.E. Paquin, J. Adams, *Nature* 306 (1983) 368.
- [18] J.B.C. Jackson, L. Buss, *Proc. Natl. Acad. Sci. USA* 72 (1975) 5160.

- [19] B. Kerr, M.A. Riley, M.W. Feldman, B.J.M. Bohannon, *Nature* 418 (2002) 171.
- [20] D. Semmann, H. Krambeck, M. Milinski, *Nature* 425 (2003) 390.
- [21] A. Szolnoki, M. Perc, *Europhys. Lett.* 92 (2010) 38003.
- [22] A. Szolnoki, G. Szabó, M. Perc, *Phys. Rev. E* 283 (2011) 036101.
- [23] J. Hofbauer, K. Sigmund, *Evolutionary Games and Population Dynamics*, Cambridge University Press, Cambridge, England, 1998.
- [24] Y.-C. Lai, Y.-R. Liu, *Phys. Rev. Lett.* 94 (2005) 038102.
- [25] L.-L. Jiang, T. Zhou, M. Perc, X. Huang, B.-H. Wang, *New J. Phys.* 11 (2009) 103001.
- [26] G.-Y. Zhang, Y. Chen, W.-K. Qi, S.-M. Qing, *Phys. Rev. E* 79 (2009) 062901.
- [27] H.-J. Shi, W.-X. Wang, R. Yang, Y.-C. Lai, *Phys. Rev. E* 81 (2010) 030901(R).
- [28] W.-X. Wang, Y.-C. Lai, C. Grebogi, *Phys. Rev. E* 81 (2010) 046113.
- [29] R. Yang, W.-X. Wang, Y.-C. Lai, C. Grebogi, *Chaos* 20 (2010) 023113.
- [30] L.-L. Jiang, T. Zhou, M. Perc, B.-H. Wang, *Phys. Rev. E* 84 (2011) 021912.
- [31] W.-X. Wang, X. Ni, Y.-C. Lai, C. Grebogi, *Phys. Rev. E* 83 (2011) 011917.
- [32] G. Szabó, *J. Phys. A: Math. Gen.* 38 (2005) 6689.
- [33] G. Szabó, A. Szolnoki, G.A. Sznaider, *Phys. Rev. E* 76 (2007) 051921.
- [34] S. Redner, *A Guide to First-Passage Processes*, Cambridge University Press, Cambridge, 2001.
- [35] D.T. Gillespie, *J. Comput. Phys.* 22 (1976) 403.
- [36] C.E. Shannon, *Bell Syst. Tech. J.* 27 (1948) 379.
- [37] A.S. Mikhailov, K. Showalter, *Phys. Rep.* 425 (2006) 79.
- [38] M. Assaf, B. Meerson, *Phys. Rev. Lett.* 497 (2006) 200602.
- [39] O. Ovaskainen, B. Meerson, *Trends Ecol. Evol.* 25 (2010) 643.
- [40] Y. Ben Zion, G. Yaari, N.M. Shnerb, *PLoS Comput. Biol.* 6 (2010) e1000643.
- [41] L.-L. Jiang, W.-X. Wang, Y.-C. Lai, B.-H. Wang, *Phys. Rev. E* 81 (2010) 036108.